Colossal permittivity properties of Zn,Nb co-doped TiO_2 with different phase structures

Xianhua Wei,[ab] Wenjing Jie,[a] Zhibin Yang,[a] Fengang Zheng,[c] Huizhong Zeng,[d] Yun Liu[e] and Jianhua Hao*[a]

[a] Department of Applied Physics, The Hong Kong Polytechnic University, Hung Hom, Hong Kong, P. R. China. E-mail: jh.hao@polyu.edu.hk; Fax: +852 23337629; Tel: +852 27664098

[b] State Key Laboratory Cultivation Base for Nonmetal Composites and Functional Materials, Southwest University of Science and Technology, Mianyang 621010, P. R. China

[c] Jiangsu Key Laboratory of Thin Films, Department of Physics, Soochow University, Suzhou 215006, P. R. China

[d] State Key Laboratory of Electronic Thin Films and Integrated Devices, University of Electronics Science and Technology of China, Chengdu 610054, P. R. China

[e] Research School of Chemistry, The Australian National University, Canberra, ACT 2601, Australia

Abstract

Colossal permittivity properties were studied in Zn,Nb co-doped TiO_2 with different phase structures. The $(Zn_{1/3}Nb_{2/3})_{0.05}Ti_{0.95}O_2$ rutile ceramics were prepared by the solid state sintering technique, while the amorphous and anatase films were respectively fabricated by a pulsed laser deposition method and a subsequent rapid thermal annealing. The ceramics showed a frequency (10^2–10^6 Hz) independent dielectric response with a colossal dielectric permittivity (B30000), and a relatively low dielectric loss (B0.05) at room temperature. The excellent colossal permittivity properties are comparable to those of the previously reported rutile TiO_2 ceramics by co-doping trivalent and pentavalent elements. For amorphous films, the dielectric permittivity decreased, and the dielectric loss increased slightly compared to those of the ceramics. Compared with the amorphous thin films, the annealed anatase ones exhibited a simultaneous increase in both dielectric permittivity and loss at low frequency while kept almost unchanged at high frequency. These results suggest that co-doping of bivalent elements with Nb into TiO_2 with various phase structures can yield colossal permittivity effects, including ultra- high dielectric permittivity, relatively low dielectric loss. Furthermore, the colossal permittivity properties may be mainly attributed to the effect of the electron-pinned defect-dipoles in Zn,Nb co-doped TiO_2 with different phase structures rather than the grain boundary capacitance effect. Besides, the frequency and bias dependent dielectric properties were also investigated in thin film forms, which could be affected by the electrode-film interface and mobile ions. Our results are helpful for not only investigating the new class of colossal permittivity materials, but also developing dielectric thin film device applications.

1. Introduction

Colossal permittivity materials have drawn much attention from the community of dielectrics due to their potential application for microelectronic devices and high-energy-density storage.[1,2] Since the beginning of this century, several candidates have been developed, including perovskite ferroelectric oxides, $CaCu_3Ti_4O_{12}$, doped NiO, and $La_{2-x}Sr_xNiO_4$.[3–7] Unfortunately, these classes of materials seem to be not ideal for straightforward application when considering the amplitude of their dielectric loss, as well as the frequency and temperature dependent dielectric properties.[1,8] Very recently, Liu's group reported the experimental evidence and provided theoretical explanation for colossal permittivity and low dielectric loss in Nb, In co-doped rutile TiO_2 ceramics.[9,10] In the new colossal permittivity materials, simultaneous donor and acceptor substitutions into TiO_2 are considered to create the local combination of a partially delocalized electron, as a result of the formation of a defect-dipole complex/cluster. Furthermore, the overall charge balance in the defect-dipole complex/cluster should play an important role in the low dielectric loss. Although the grain boundary capacitance effect is considered to contribute to the colossal dielectric properties,[11,12] the newly discovered co-doped TiO_2 materials would provide more choices to tune and optimize dielectric properties through the combination of substituted ions. To date, colossal permittivity properties have also been confirmed in a series of rutile TiO_2 ceramics by co-doping trivalent (In, Pr, Dy, Sm, Gd, Yb, Ga, Al, or Sc) and pentavalent cations (Nb, Sb, or Ta) with equivalent stoichiometric proportion.[13–15] Therefore, it should be feasible that co-doping of monovalent or bivalent elements with Nb into TiO_2 may also

lead to colossal permittivity effects on the conditions under which the charge balance is kept.

Actually, in some piezoelectric ceramics with an ABO_3 perovskite structure, the solid solubility of Zn,Nb into Ti sites is large.[16] This provides us an opportunity to use Zn and Nb as co-doping elements into TiO_2. However, the colossal dielectric properties have not been achieved in any bivalent ions and Nb co-doped TiO_2 ceramics or thin films. In addition, amorphous Nb, In co-doped rutile TiO_2 thin films deposited by pulsed laser deposition (PLD) at room-temperature also exhibited a relatively high permittivity.[17] It can overcome the problem of excessively high temperature treatment of the rutile phase, and would be favorable for the integration of electronic devices. Considering the polymorphic phase transition among the TiO_2 crystal structures, it is essential to clarify the existence of defect dipoles by extensively investigating the colossal dielectric effects in both ceramics and thin films with different phase structures. In this work, Zn,Nb co-doped TiO_2 samples in the form of rutile ceramics, amorphous films, and anatase films were fabricated. We systematically studied the dielectric properties of Zn,Nb co-doped TiO_2 with different phase structures. The results indicate that co-doping of the bivalent elements with Nb into TiO_2 can yield colossal permittivity effects regardless of the phase of TiO_2 due to the effect of the electron-pinned defect-dipoles.

2. Experimental

The ceramics were prepared using a conventional solid state reaction method. A proportionate amount of starting materials of ZnO, Nb_2O_5, and TiO_2 with analytical grade purity was weighted according to the stoichiometry of $(Zn_{1/3}Nb_{2/3})_{0.05}Ti_{0.95}O_2$. The ceramics were fabricated by ball milling, calcinations, pressing, and sintering. Thin films were deposited by PLD on Pt/Si substrates with an operation wavelength of KrF (l = 248 nm). Thin film deposition was made at substrate temperature below 300 1C in a dynamic oxygen atmosphere (2 Pa) with a laser energy density of about 2 J cm^{-2}. Film thickness was about 700 nm estimated from the laser pulses and the deposition rate, which could be further confirmed by the cross sectional analysis of scan electron microscopy (SEM). Amorphous films were crystallized by RTA (Hefei Kejing OTF-1200X-4-RTP) treatment at 600 1C for 1 min with a heating rate of 30 1C s^{-1} under a N_2 atmosphere. An X-ray diffractometer (XRD) (Rigaku, SmartLab) was employed to analyze the crystalline structure. The vibrational properties of samples were characterized by Raman spectroscopy (HORIBA, HR800) excited by 488 nm laser with a spot size of about 1 mm. To construct parallel-plate capacitors, the ceramics were pasted with silver on both sides, while for the films a top Au electrode with a radius of 100 micrometer was covered with a shadow mask and deposited by thermal evaporation. The dielectric behaviors of the capacitors were measured using an Impedance Analyzer (Agilent E4980A) from 100 to 2 MHz as a function of frequency at room temperature. All the dielectric measurements were performed at room temperature in air ambience.

3. Results and discussion

Fig. 1 presents the XRD patterns of ceramics and thin films. The ceramics have a rutile crystal structure except for a secondary phase of $ZnTiO_3$, which is similar to the reported In doping into TiO_2 at the doping level beyond 1%.[9] On the other hand, there are no diffraction peaks of any TiO_2 crystalline phase in the XRD results for the thin films deposited below 300 1C, except for those from the Si substrate, the Pt bottom electrode and the Au top electrode. It reveals that the films are amorphous, which is in agreement with previous results that amorphous TiO_2 films were obtained at low deposition temperature.[17,18] After annealing, the diffraction peaks of the anatase structure were found, suggesting that the films were finally converted to the anatase phase by treating with RTA.

Fig. 2 presents the surface morphology of co-doped TiO_2 with different phase structures. The rutile ceramics were clearly observed to possess a dense microstructure as shown in the SEM image of Fig. 2(a). In addition, Fig. 2(b) and (c) show the comparison of the AFM images from the films within a scan area of 500 Â 500 nm^2 before and after annealing. For the amorphous films, the surface shows a smooth morphology without observable grains or grain boundaries. For the annealed films, the grain size is about 40 nm, and the magnitude of the surface roughness increases.

Raman spectroscopy can further determine the microstructure difference between ceramics and films as shown in Fig. 3. There are four peaks centered at 142 cm^{-1} (B_{1g}), 240 cm^{-1} (the second-order scattering), 445 cm^{-1} (E_g), and 611 cm^{-1} (A_{1g}) in the Raman spectrum of the rutile ceramics. It was reported that the four Raman peaks were found in nanocrystalline rutile TiO_2 with crystallite sizes down to 5 nm.[19] This can further conclude that the ceramics are in the rutile phase. In contrast, there are only two large and broad bumps at about 150 cm^{-1} and 590 cm^{-1} in the Raman spectra of the thin films deposited at low temperature. They are very close to those Raman peaks of crystalline TiO_2 (anatase: Eg; rutile: B_{1g}, A_{1g}). It is caused by the presence of a short range order in the amorphous films.[17] After annealing, five peaks centered at 146, 197, 395, 518, 638 cm^{-1} can be assigned as E_g, E_g, B_{1g}, B_{1g}, and E_g modes of the anatase phase, respectively. The strongest E_g mode at 146 cm^{-1} arising from the external

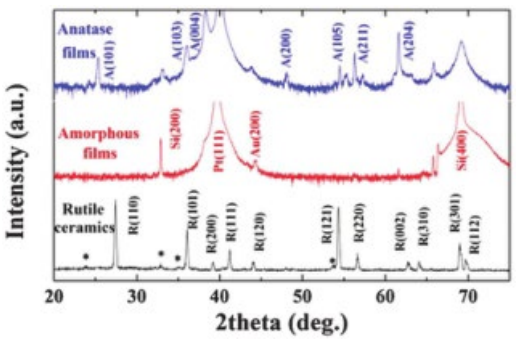

Fig. 1 XRD patterns of rutile ceramics, amorphous and anatase thin films of $(Zn_{1/3},Nb_{2/3})_{0.05}Ti_{0.95}O_2$. A stands for the anatase phase, while R for rutile and the asterisks for $ZnTiO_3$.

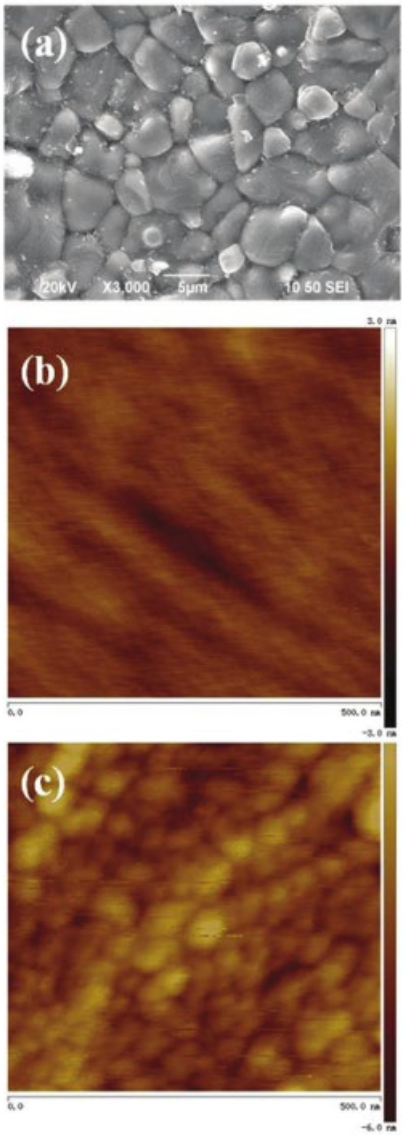

Fig. 2 Surface morphology of $(Zn_{1/3},Nb_{2/3})_{0.05}Ti_{0.95}O_2$; (a) the SEM image of rutile ceramics; (b) the AFM image of amorphous thin films; (c) the AFM image of anatase thin films.

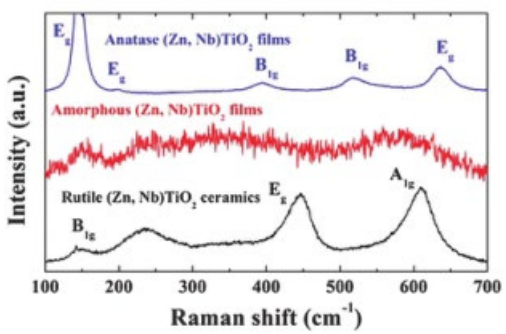

Fig. 3 Raman spectra of rutile ceramics, amorphous and anatase thin films $(Zn_{1/3},Nb_{2/3})_{0.05}Ti_{0.95}O_2$.

vibration of the anatase structure is well resolved.[20] It indicates that an anatase phase long-range order is formed. Besides, when considering that the spot size of laser is about 1 mm in Raman measurements, the absence of Raman feature peaks arising from ZnO or Nb_2O_5 in all samples also suggests that the dopants of Zn,Nb should be incorporated into the lattice of TiO_2 rather than the formation of additional dopants of ZnO or Nb_2O_5. This is consistent with the aforementioned XRD results as shown in Fig. 1.

Fig. 4 shows the dielectric permittivity and loss as a function of measuring frequency for the ceramics and films. The permittivity of the ceramics decreases slowly from about 3.3 Â 10[4] to 2.6 Â 10[4] while the frequency increases from 10^2 to 10^6 Hz. Meanwhile, their dielectric loss keeps very low about 0.03 to 0.05 at a frequency of 10^2 to 10^5 Hz, and shows a slight increase of up to 0.07 at 10^6 Hz. The results suggest that excellent dielectric properties can be achieved in the Zn,Nb co-doped ceramics with a colossal dielectric permittivity and a low loss. More importantly, a good frequency-stability of dielectric characteristics is apparent in the doped TiO_2 ceramics, which is beneficial to practical applications. Furthermore, the dielectric properties of the Zn,Nb co-doped ceramics are comparable to those found in trivalent element doped Nb:TiO_2 ceramics.[9–13] It indicates that the defect dipole might also be valid in the Zn,Nb co-substitution of Ti in the TiO_2 systems.

It has been reported that doping only with Nb can also increase the permittivity of TiO_2 with the same magnitude order as that of (In,Nb) co-doped TiO_2. However, its dielectric loss is relatively high due to the delocalized electron transport related interfacial polarization. The formation of a delocalized

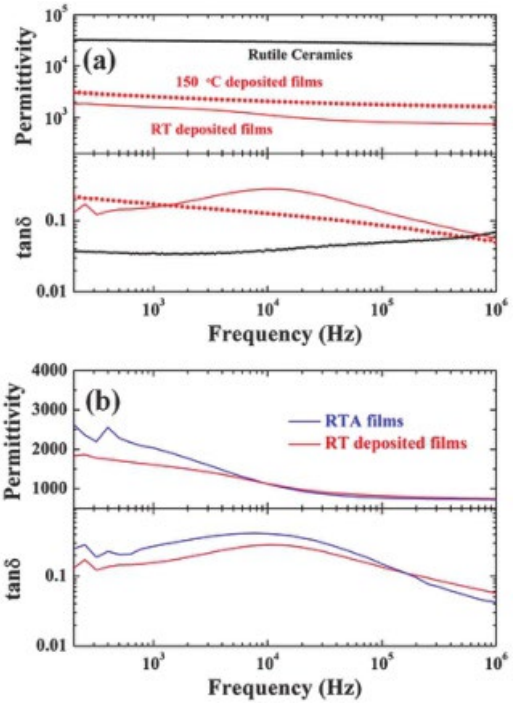

Fig. 4 (a) Dielectric properties as a functionof frequency in $(Zn_{1/3},Nb_{2/3})_{0.05}Ti_{0.95}O_2$ rutile ceramics and amorphous thin films deposited at room temperature and 150 1C; (b) comparison of dielectric properties of amorphous and anatase thin films.

electron can be expressed as follows

$$Nb_2O_5 \xrightarrow{2TiO_2} 2Nb_{Ti}^{\bullet} + 4O_O + 2e' + Ti_{Ti}^{0} + \frac{1}{2}O_2 \uparrow \quad (1)$$

where $Nb_{Ti}^{\bullet}$ represents Nb on the Ti lattice site, O_O on the lattice site. In Zn,Nb co-doped TiO_2, the incorporating of the acceptor ZnO would lead to the formation of oxygen vacancies.

$$ZnO \xrightarrow{TiO_2} Zn_{Ti}'' + O_O + V_O^{\bullet\bullet} \quad (2)$$

where Zn_{Ti}'' is Zn on the Ti lattice site, and $V_O^{\bullet\bullet}$ is the oxygen vacancy. In titanate dielectric materials, the incorporation of acceptor dopants, such as Mn or Co replacing Ti^{4+} could induce a decrease in electron concentration and the formation of a defect complex $(Mn_{Ti}'' V_O^{\bullet\bullet})^{\times}$.[21,22] They separately contribute to a lower dielectric loss and a higher dipole moment density, which is also expected in this work.

Since the ratio of Zn:Nb was designed to be 1:2 in this work, the amount of oxygen vacancies and electrons in eqn (1) and (2) would be equal. For this case, complex clusters among Zn_{Ti}'', $V_O^{\bullet\bullet}$, $Nb_{Ti}^{\bullet}$, and Ti_{Ti}^{0} are expected from the viewpoint of low energy configuration. In (Nb,In) co-doped rutile TiO_2 samples, there are two possibilities to correlate the lowest energy structures of the diamond $Nb_2^{5+}Ti^{3+}A_{Ti}$ and triangle defects $In_{3}'V_O^{\bullet\bullet}Ti_{3}'$.[9] If the diamond and triangle defects are overlapped, the A atom of the diamond structure could be Ti^{3+} or In^{3+}. More defect clusters might be isolated due to the small doping content, and the A site becomes Ti^{4+}. Similarly, it can be speculated that the combinations of the two types of defect clusters could, respectively, be $Nb_{2}^{5}{}'Ti_{2}^{3}{}'Ti_{2}^{3}{}'V_O^{\bullet\bullet}Zn_2'$ and $Nb_5'Ti_3'Ti_4'Ti_3'Ti_4'V_O^{\bullet\bullet}Zn_2'$ for overlapped and isolated cases, as shown in Fig. 5(a). As a consequence, large defect-dipole clusters with the high localized electrons induced by these complexes are responsible for the colossal permittivity and low dielectric loss. Actually, additional Nb should induce the independent reduction of Ti^{4+} due to the presence of the secondary phase $ZnTiO_3$. The effect of doping concentrations on the dielectric properties needs further investigation.

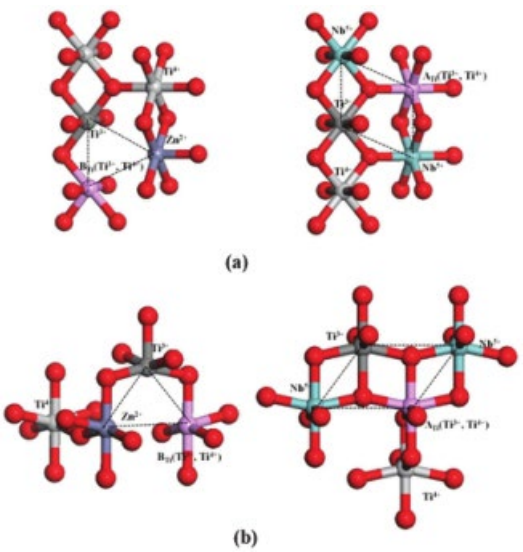

Fig. 5 Schematic structure of possible defect complexes in Zn,Nb co-doped TiO_2: (a) rutile phase; (b) anatase phase.

In order to investigate the underlying mechanism regarding electron-pinned defect-dipoles, the dielectric properties of amorphous and anatase Zn,Nb co-doped TiO_2 films were further investigated. For the samples deposited at 150 1C, the dielectric permittivity and loss are about 1780 and 0.08 at 100 kHz, respectively. When the measuring frequency was set to the highest value of 2 MHz, the dielectric permittivity and loss were decreased to 1600 and 0.035, respectively. A similar tendency can be found in those room-temperature deposited samples, which show an even lower dielectric permittivity of about 1000. The reason responsible for improving dielectric properties of the films grown at higher substrate temperature might be associated with some factors, such as contact resistance, interface characteristics as well as better adhesion between the bottom electrode and the film. In fact, it has been reported that the adhesion of PLD coatings could be improved by raising the substrate temperature.[23] At any rate, compared with the relatively small dielectric permittivity (usually below 200) and quite high dielectric loss of pure amorphous TiO_2 films, a significant improvement of dielectric properties was found in our amorphous co-doped TiO_2 films. Due to the absence of grain boundaries in amorphous thin films, the colossal dielectric effect is ascribed to defect complexes or clusters in the short range at the atomic level, which can rule out the possible role played by the grain boundary capacitance effect contributing to the colossal dielectric properties. For the grain boundary capacitance effect, delocalized electrons range over a large distance in the grain. It would cause the electron responses at low frequency, and the dielectric loss would be large at high frequency.[17] At high frequency, their relative low loss in this work makes them possible in the application of microelectronic devices.[17,24]

Fig. 4(b) demonstrates the effect of ex situ RTA treatment on dielectric properties of the fabricated samples. There is no obvious difference between the two samples at high frequency, while the permittivity and loss increase for the RTA sample at low frequency. Herein, we can conclude that colossal dielectric properties have been confirmed in amorphous, anatase and rutile Zn,Nb co-doped TiO_2. In other words, similar electron-pinned dipoles by defect complexes should be effective in the co-doped TiO_2 with different phase structures. For example, triangular $M_1M_2M_3V_O$ (M = metal ions, Zn, Ti) and polygon or polyhedron clusters composed of Nb and Ti could be correlated in the anatase structure. Since the coordination of oxygen is 3 in both phases, the three metal ions around oxygen vacancies would form isosceles triangular clusters. A slight distortion can be found between the two isosceles triangular clusters in anatase and rutile phases. A similar distortion may exist between those clusters composed of Nb and Ti in the two phases. The schematic structure of possible defect complexes in anatase TiO_2 is shown in Fig. 5(b).

The dielectric properties of the films are inferior to those of their bulk counterparts. Moreover, both the permittivity and loss decrease while the frequency increases, suggesting that there might be other factors influencing the dielectric response

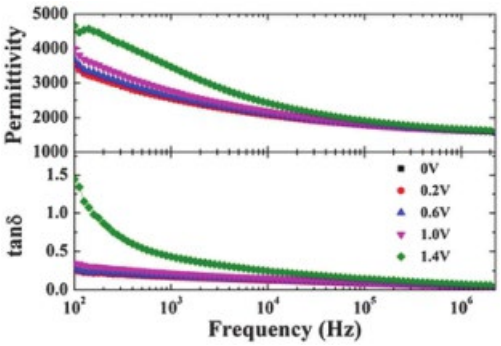

Fig. 6 Frequency dependence of the dielectric permittivity and loss of amorphous $(Zn_{1/3},Nb_{2/3})_{0.05}Ti_{0.95}O_2$ thin films deposited at 150 1C under different dc biases.

in the amorphous films. Fig. 6 presents the relationships between the dielectric properties of the 150 1C deposited films and the direct current (dc) bias and conduction. Both the dielectric permittivity and loss increase with the increase of the applied dc bias, particularly at low frequency. The dielectric properties in the low-frequency regime are generally related to the impurity, defect, and space-charge carrier transport processes.[25] In this work, there should be some amount of oxygen vacancies existed in the films deposited by PLD, due to the Zn doping effect and low oxygen ambience.[26] Based on the polaron nature of dielectric relaxation in bulk TiO_2 ceramics near room temperature, electron can hop between Ti^{4+} and Ti^{3+} ions due to the existence of oxygen vacancies.[27] Since the hopping motions of localized carriers yield bulk dielectric response, the spectroscopic plot of dielectric loss is expected to be independent of d.c. bias. However, the dc bias stress-induced modification of the capacitance only at low frequency (Fig. 6) indicates that the extra mechanism may play a role. The defect creation or charge trapping was ever found to cause capacitance variations in HfO_2 films.[28] In $KNbO_3$ ceramics, similar results can be explained by electrode-specimen contribution.[29] Therefore, it is speculated that the bias leads to trapped charge at defects close to interfaces between the electrode and thin films. Due to the interface polarization, the capacitance is enhanced at low frequency, and remains almost unchanged at high frequency since it cannot follow the change of the high-frequency electric field.

4. Conclusion

In conclusion, Zn,Nb co-doped TiO_2 can yield colossal permittivity properties in the forms of rutile ceramics, amorphous and anatase thin films. The ceramics show a frequency-independent dielectric response with a colossal dielectric permittivity and a very low dielectric loss. In comparison with the corresponding ceramics, both the amorphous and anatase thin films exhibit a decreased dielectric permittivity and a slight increased dielectric loss. It is suggested that the co-doping of bivalent elements with Nb into TiO_2 can give rise to colossal permittivity effects regardless of the phase of TiO_2 on conditions under which the charge balance is kept. The defect clusters with balanced charge are responsible for the colossal permittivity effect by co-doping bivalent elements with Nb into TiO_2 with different phase structures. Consequently, this work will benefit for not only investigating the fundamental properties of the new colossal permittivity materials, but also developing dielectric thin film device applications.

Acknowledgements

This work was supported by the grant from Research Grants Council of Hong Kong (GRF No. PolyU 153004/14P).

Notes and references

1 P. Lunkenheimer, S. Krohns, S. Riegg, S. G. Ebbinghaus, A. Reller and A. Loidl, Eur. Phys. J.: Spec. Top., 2010, 180, 61.
2 C. C. Homes and T. Vogt, Nat. Mater., 2013, 12, 782.
3 M. T. Buscaglia, M. Viviani, V. Buscaglia, L. Mitoseriu, A. Testino, P. Nanni, Z. Zhao, M. Nygren, C. Harnagea, D. Piazza and C. Galassi, Phys. Rev. B: Condens. Matter Mater. Phys., 2006, 73, 064114.
4 M. A. Subramanian, D. Li, N. Duan, B. A. Reisner and A. W. Sleight, J. Solid State Chem., 2000, 151, 323.
5 C. C. Homes, T. Vogt, S. M. Shapiro, S. Wakimoto and A. P. Ramirez, Science, 2001, 293, 673.
6 J. B. Wu, C. W. Nan, Y. H. Lin and Y. Deng, Phys. Rev. Lett., 2002, 89, 217601.
7 S. Krohns, P. Lunkenheimer, Ch. Kant, A. V. Pronin, H. B. Brom, A. A. Nugroho, M. Diantoro and A. Loidl, Appl. Phys. Lett., 2009, 94, 122903.
8 J. H. Hao, W. D. Si, X. X. Xi, R. Y. Guo, A. S. Bhalla and L. E. Cross, Appl. Phys. Lett., 2000, 76, 3100.
9 W. B. Hu, Y. Liu, R. L. Withers, T. J. Frankcombe, L. Nore´n, A. Snashall, M. Kitchin, P. Smith, B. Gong, H. Chen, J. Schiemer, F. Brink and J. Wong-Leung, Nat. Mater., 2013, 12, 821.
10 W. B. Hu, K. Lau, Y. Liu, R. L. Withers, H. Chen, L. Fu, B. Gong and W. Hutchison, Chem. Mater., 2015, 27, 4934.
11 J. L. Li, F. Li, C. Li, G. Yang, Z. Xu and S. J. Zhang, Sci. Rep., 2015, 5, 8295.
12 J. L. Li, F. Li, Y. Y. Zhuang, L. Jin, L. H. Wang, X. Y. Wei, Z. Xu and S. J. Zhang, J. Appl. Phys., 2014, 116, 074105.
13 X. J. Cheng, Z. W. Li and J. G. Wu, J. Mater. Chem. A, 2015, 3, 5805.
14 W. Tuichai,P.Srepusharawoot,E.Swatsitang,S.Danwittayakuld and P. Thongbai, Microelectron. Eng., 2015, 146, 32.
15 Z. W. Li, J. G. Wu and W. J. Wu, J. Mater. Chem. C, 2015, 3, 9206.
16 M. K. Durbin, E. W. Jacobs, J. C. Hicks and S.-E. Park, Appl. Phys. Lett., 1999, 74, 2848.
17 Z. G. Gai, Z. X. Cheng, X. L. Wang, L. L. Zhao, N. Yin, R. Abah, M. L. Zhao, F. Hong, Z. Y. Yu and S. X. Dou, J. Mater. Chem. C, 2014, 2, 6790.
18 X. Xiao, W. Wang, S. Li, Y. Liu, D. Zhang, S. Qiang, X. Gao and B. Zhang, Chin. J. Lasers, 2013, 140, 0207001.

19 V. Swamy, B. C. Muddle and Q. Dai, Appl. Phys. Lett., 2006, 89, 163118.
20 W. F. Zhang, Y. L. He, M. S. Zhang, Z. Yin and Q. Chen, J. Phys. D: Appl. Phys., 2000, 33, 912.
21 W. J. Jie, J. Zhu, W. F. Qin, X. H. Wei, J. Xiong, Y. Zhang, A. Bhalla and Y. R. Li, J. Phys. D: Appl. Phys., 2007, 40, 2854.
22 S. Li, H. Z. Zeng, S. Y. Zhang and X. H. Wei, Appl. Phys. Lett., 2013, 102, 153506.
23 J. Tang, J. S. Zabinski and J. E. Bultman, Surf. Coat. Technol., 1997, 91, 69.
24 Y. Lin, Y. B. Chen, T. Garret, S. W. Liu, C. L. Chen, L. Chen, R. P. Bontchev, A. Jacobson, J. C. Jiang, E. I. Meletis, J. Horwitz and H.-D. Wu, Appl. Phys. Lett., 2002, 81, 631.
25 S. J. Lee, K. Y. Kang and S. K. Han, Appl. Phys. Lett., 1999, 75, 1784.
26 W. J. Kim, W. Chang, S. B. Qadri, J. M. Pond, S. W. Kirchoefer, D. B. Chrisey and J. S. Horwitz, Appl. Phys. Lett., 2000, 76, 1185.
27 C. C. Wang, N. Zhang, Q. J. Li, Y. Yu, J. Zhang, Y. D. Li and H. Wang, J. Am. Ceram. Soc., 2015, 98, 148.
28 O. Khaldi, P. Gonon, C. Mannequin, C. Valle´e, F. Jomni and A. Sylvestre, ECS Solid State Lett., 2013, 2, N15.
29 S. U. Sharath, R. K. Singh, Raghvendra, B. P. Singh, P. Kumar and P. Singh, J. Am. Ceram. Soc., 2013, 96, 3127.